


RESEARCH ARTICLE

Verb generation for presurgical mapping: Gaining specificity

Elena Salillas¹  | Concetta Luisi² | Giorgio Arcara³ | Elif Nur Varlı⁴ | Domenico d'Avella⁵ | Carlo Semenza⁴

¹Department of Psychology and Sociology, Universidad de Zaragoza, Zaragoza, Spain

²Neurology, Epilepsy and Movement Disorders, Bambino Gesù Children's Hospital, IRCCS, Full Member of European Reference Network EpiCARE, IRCCS, Rome, Italy

³IRCCS San Camillo Hospital, Venice, Italy

⁴Padova Neuroscience Center, University of Padova, Padova, Italy

⁵Academic Neurosurgery, Department of Neuroscience, University of Padova, Padova, Italy

Correspondence

Elena Salillas, Department of Psychology and Sociology, Universidad de Zaragoza, Zaragoza, Spain.

Email: esalillas@unizar.es

Funding information

H2020 Marie Skłodowska-Curie Actions, Grant/Award Number: 793071

Abstract

Verb generation is among the most frequently used tasks in presurgical mapping. Because this task involves many processes, the overall brain effects are not specific. While it is necessary to identify the whole network involving noun comprehension or semantic retrieval and lexical selection to produce the verb, isolation of those components is also crucial. Here, we present data from four patients undergoing presurgical brain mapping. The study implied a reanalysis of magnetoencephalography data with a recategorization of the used items. It aimed to extract the task component that relies on the inferior frontal gyrus (IFG). The task could be applied with higher specificity when targeting frontal areas. For that, we based item classification on the selection demands imposed by the noun. It is a robust finding that the IFG carries out this selection and that a quantitative index can be calculated for each noun, which depends on the selection effort (*Proceedings of the National Academy of Sciences of the United States of America*, 1997; **94**(26):14792–14797, *Proceedings of the National Academy of Sciences of the United States of America*, 1998; **95**(26):15855–15860). Data showed focality and specificity, with a correlation between this derived index and source activations in the inferior frontal gyrus for all patients. Strikingly, we detected when the right-hemisphere homologue area was involved in the selection process in two patients showing reorganization or language right lateralization. The present data are a step towards a dissection of broad specific tasks frequently used in presurgical protocols.

KEYWORDS

Broca's area, frontal lobe, lexical selection, magnetoencephalography, presurgical mapping, verb generation task

This is an open access article under the terms of the [Creative Commons Attribution-NonCommercial-NoDerivs](https://creativecommons.org/licenses/by-nc-nd/4.0/) License, which permits use and distribution in any medium, provided the original work is properly cited, the use is non-commercial and no modifications or adaptations are made.

© 2023 The Authors. *Journal of Neuropsychology* published by John Wiley & Sons Ltd on behalf of The British Psychological Society.

INTRODUCTION

One of the four most used tasks in presurgical mapping is the verb generation task (VG; Black et al., 2017). It is included in the mapping protocol when addressing the prefrontal areas (Rofes & Miceli, 2014). Neurocognitive research emphasizes the role of prefrontal structures in verb processing (Bastiaanse & Jonkers, 2007; Damasio & Tranel, 1993; Mätzig et al., 2009; Miceli et al., 2007; Pillon & d'Honinchtun, 2011; Shapiro & Caramazza, 2003).

VG is commonly used to map cortical areas involved in lexicosemantic processes when frontal or temporal regions are targeted. During this task, the participant must covertly emit a verb upon a given noun. The task implies a set of processes: the patient must first read (or listen to) the noun and comprehend its meaning to generate an associated verb. Semantic knowledge must be accessed first, and lexical selection must be applied to possible alternatives. The multicomponent nature of the VG task makes activations unspecific, and the concrete roles of the different regions within the network are left unknown for a given patient. While it is helpful to know the complete set of areas behind VG, a knowledge of the specific roles of each region during this task is valuable: many times, frontal lobes can be targets for surgery, with spared temporal lobes.

In healthy participants and at the group level, this task activates frontotemporal regions, including the inferior frontal gyrus (IFG) and the middle and superior temporal gyri (Allendorfer et al., 2012; Cerliani et al., 2016; Grè & Decety, 2001). Neurosynth-based meta-analysis shows a left frontotemporal network (Cirillo et al., 2022). However, at the single-case level, the activated areas are notably broader (Cirillo et al., 2022; Pang et al., 2011), something detrimental to the goals of presurgical mapping.

Here, we present an effort to use what is known in the literature behind the VG task to achieve higher focality in mapping the IFG at the single-case level. One starting point is to focus on the lexical selection component of the VG task. Thompson-Schill et al. (1997, 1998) already explored this task very precisely. They robustly showed that stroke patients with IFG damage failed in this task but only with specific nouns. Setting aside the IFG as a basis for semantic retrieval, these authors proposed the IFG as a region involved in lexical selection during VG. Patients with IFG did not fail to generate a verb after nouns such as SCISSORS; they, however, systematically failed to generate a verb after nouns such as WHEEL. The difference between these two nouns, as stimuli for VG, is that scissors will elicit the verb CUT without semantic competition. Still, WHEEL will require a process of resolution to that competition. For this last noun, there is more variability in the verbs to be emitted (*i.e.*, TURN; TWIST). The IFG, according to the authors, serves to bias this competition during VG and, more generally, during language production. Note that other authors (Martin & Yan, 2006; Wagner et al., 2001) re-interpreted the results in terms of association strengths between cues (the noun) and target (the verb). However, the consequences for mapping do not change because differences between the two types of nouns should nevertheless be found. And, as we will see, the index proposed by Thompson-Schill and collaborators is centred on the cue, regardless of the target, allowing a free emission of any target by the patient.

The present study aims, first, to adjust the VG task in a way that one can specifically target the IFG in the individual patient. Second, such adaptation should be helpful in cases where brain reorganization might have occurred due to different causes (*e.g.* tumour growth or epilepsy-related plasticity). Functionally equivalent recruited areas should be detectable by the task in surrounding regions to the IFG or contralaterally, in the right IFG (Tracy & Osipowicz, 2011). Similarly, the task should also be sensitive to the right lateralization of language functions. For that, we retrospectively classified the nouns included in three VG paradigms already used for the presurgical mapping with magnetoencephalography (MEG); despite the surgeries not always targeting the frontal lobe, the retrospective analyses aimed to exemplify specificity in four individual cases. We adapted three different paradigms that used different sets of nouns. Items were labelled according to the selection demands imposed by the noun. The brain sources for four patients for those items were obtained by observing the brain areas that responded to the increment of selection demands during the VG task.

METHOD

Participants

The study involves four patients: two tumour patients, one patient with cavernous angioma and one early-onset epilepsy patient. They were admitted to IRCCS San Camillo Hospital (Venice, Italy) for MEG-based language mapping before surgery. All patients were native Italian speakers. The study was approved by the pertinent Ethical Committee of the IRCCS San Camillo Hospital and was performed under the approved guidelines. All methods followed the Declaration of Helsinki. All patients signed informed consent.

Patient L

Patient L was a 25-year-old male with oligodendroglioma in the left temporal lobe. As symptoms, he exhibited repeated episodes of focal-to-bilateral tonic-clonic seizures induced by the tumour.

Patient A

Patient A was a 38-year-old female with a left frontal cavernous angioma (cingulum). As symptoms, she exhibited 6 years of intense headaches followed by nausea, which worsened in the period previous to surgery.

Patient S

Patient S was a 14-year-old female with no previous history of neurosurgery. She had early-onset left temporal lobe epilepsy associated with hippocampal sclerosis, in which symptoms started at 3 years of age. In addition, she had acute lymphocytic leukaemia, and she received chemotherapy. After posterior reversible encephalopathy syndrome (PRES) and status epilepticus involving left temporo-parieto-occipital areas, the patient lost language abilities and then reacquired them.

Patient G

Patient G was a 53-year-old female. She had a history of an ovarian tumour that was surgically treated 8 years before the time of the examination. A brain tumour initially classified as a metastasis was found in the left temporal lobe after a medical investigation following the patient's complaint of frequent headaches. The brain tumour was later classified as a low-grade glioma, unrelated to the preceding tumour, in the left temporal lobe.

Stimuli reclassification

Two pools of 100 nouns from already implemented verb selection MEG paradigms were classified according to their selection constraints, as suggested by Thompson-Schill et al. (1997). The study aimed to refine already applied paradigms by reclassifying the used items. The lists of items differed for one of the patients (S). For item classification, we created a questionnaire with the nouns and asked healthy participants to emit a verb for each noun. Different groups of participants were chosen for the items

from each patient: 18 participants (average 21 y.o.; 5 males) for patients L, G, and A and 12 participants for Patient S (average age 24 y.o., 6 males).

A *selectivity ratio calculation* was performed for the nouns: the numerator was the number of participants (NP) giving the most frequently answered verb, and the denominator was the number of participants giving the second-most frequently answered verb. Hence, for each noun:

$$\text{Selectivity ratio} = (\text{NP for the first most given verb}) / (\text{NP for the second most given verb})$$

The larger the ratio between the most frequently answered verb and the second most frequently answered verb, the lower the selection effort imposed by the noun. The largest ratio meant that most participants had given the same verb; hence, the selection effort was low. In low selection items, a higher variability of emissions occurred, meaning that the effort of selection between alternatives was higher. Hence, larger ratios were related to lower selection and smaller ratios to higher selection.

An example of low selection was *aereo* (plane), with the most frequently given response *to fly* (ratio: 17). An instance of middle selection was *braccio* (arm), with the most given answer *to hug* (ratio: 3). An example of high selection was *bottone* (button) with the same number of responses of *button up* and *to sew* (ratio: 1). The used stimuli together with the ratio associated with each noun is listed in the Appendix A. Given that the nouns were not specifically generated for this study, for one of the lists (Patient S), the selectivity ratio correlated with the noun frequency (Laudanna et al., 1995) for the initial list (absolute frequency: $r = .2$; $p = .045$; relative frequency: $r = .2$; $p = .048$). However, the ratio was not correlated with frequency for the final items remaining after artefact rejection. In the noun list used with the other three patients, ratios were not correlated with frequency. Hence, any ratio-related effect could not be explained by noun frequency.

Experimental procedure

The four retrospectively analysed experiments were implemented in Psychopy software (version 2.8.4, Peirce, 2007). The sessions began with an explanation of the task and the presentation of five training items to make sure the participant understood the procedure. Each patient performed similar verb generation tasks, yet the exact procedure slightly varied.

Patients L and G

At the beginning of each trial, a fixed sound (300 ms) was presented that clued the presentation of a new noun. The noun was presented auditorily (~1500 ms). After the end of the word, the participant could emit the verb covertly, and the trial lasted until the response. Trials were separated by a 5 s inter-trial interval.

We measured the length in ms for each auditory noun using Audacity software (Audacity® software is copyright © 1999–2021 Audacity Team) and considered the time of each word ending as the event trigger for the MEG analyses.

Patient A

A performed a similar paradigm to L and G, yet the stimuli were presented visually as written words. Hence, the fixed sound (300 ms) preceded a noun presented visually for 1500 ms. The patient was requested to emit the verb upon presenting the noun. Trials were separated by a 5 s inter-trial interval. The visual word presentation was the event trigger for the MEG analyses.

Patient S

S performed an equivalent auditory paradigm with a slight modification. While the patient fixated on a central cross, a cue sound (300 ms) preceded the auditory noun (~1000 ms). Immediately after the noun sound, a visual cue (200 ms) prompted the covert emission of the verb. The trigger for MEG analyses was set at the time of this visual cue. Trials were separated by an inter-trial interval of 2 s.

Data acquisition

Structural data (MRI) acquisition

A T1-weighted magnetic resonance image (MRI) was collected for all patients. The MRI machine used to acquire the images was a 3T Ingenia CX Philips scanner. The parameters used for a 3D sagittal T1-weighted scan were as follows: repetition time = 8.3 ms, echo time = 4.1 ms, flip angle = 8, matrix resolution = 288 Å ~ 288 and slice thickness = .87 mm.

MEG data acquisition

A 275 gradiometer CTF-MEG system (MISL) was used for MEG recordings, which was in a magnetically shielded room. Participants were prepared before entering the magnetically shielded room. Three head coils were used to calculate head position during recording. Vertical electrooculogram (VEOG; left and right), horizontal electrooculogram (HEOG; left and right) and electrocardiogram (bipolar montage) were placed to detect and correct eye movements and heartbeats in the magnetic signal. Fast-Track Polhemus hardware connected to Brainstorm software (Tadel et al., 2011) was used to digitize between 60 and 70 head points, defining the shape of the head, nose and eyebrows.

During the test, the patients remained seated with their heads stabilized within the MEG helmet using two pieces of foam. A CTF Continuous Head Localization System monitored the head position during the procedure. The screen displaying the stimuli was located 40 cm from the participant's face with a 2.5° angle. The patients listened to the stimuli through earphones. Continuous MEG signal was sampled at 1200 Hz with an online antialiasing filter at 400 Hz. Initially, MEG data were recorded as a series of sorted 1-s epochs and then transformed into a continuous signal for data analysis. Third-order gradient correction was applied in real time to extend MEG detectors' sensitivity in response to weak signals and cancel environmental noise.

Data analysis procedure

Sensor space

Data analysis was performed with Brainstorm 2023 (Tadel et al., 2011), running on MATLAB 2022b (The MathWorks Inc., 2022), which is documented and freely available for download online under the GNU general public licence (<http://neuroimage.usc.edu/brainstorm>). Raw data were band-pass filtered (1–30 Hz). Blinks and cardiac artefact topographies were automatically detected and corrected through signal-space projection (SSP). For the cardiac artefacts, the SSP was applied in a time window of ± 40 ms, with a frequency band between 13 and 40 Hz, and for ocular artefacts, the SSP was used in a time window of ± 200 ms, with a frequency band between 1.5 and 15 Hz. Simultaneous artefacts (*i.e.* cardiac and ocular) were removed before artefact correction. After artefact automatic correction, trials containing surrounding artefacts were rejected based on visual inspection.

The existing triggers in the signal were exported according to their time of occurrence in the magnetic signal. They were matched with the order of occurrence in the log file from the experimental controller software (Psychopy). Then, they were assigned the ratio and classified and used for correlational analyses at the sensor and source levels. The recorded triggers were then imported into the magnetic signal. The signal was then segmented 100 ms before (baseline) and 1000 ms after the events, averaged for high–mid–low selection conditions. After artefact rejection, the average selection ratios for the trials entered into the sensor and source analyses were as follows: 4.3 (max: 18; min 1) for Patient L, with 99 trials; 4.83 (max: 18; min 1) for Patient A, with 55 trials; 4.89 (max: 12; min 1) for Patient S, with 67 trials; and 4.3 (max: 7.5; min 1) for Patient G, with 61 remaining trials.

The ERFs were visually inspected, overlapping the three averaged conditions across sensor clusters covering the whole head. This exploration revealed a slow wave starting approximately 200 ms after the end of the visual prompt to response (S), upon the visual word (A), or after the auditory stimulus (L and I). For L, G and A, a positive slow wave was modulated by the degree of selection, again with increasing (positive) amplitude as the selection constraints increased. For S, the degree of selection imposed by the noun evoked an increasing negative amplitude as the selection constraints increased. The functional meaning of the slow ERFs is comparable: their amplitude varied linearly according to the selection demands.

We computed the difference between the selection conditions (high–low, high–medium and medium–low) for further visual analyses. Then, we averaged these differences into three different latency bands along the observed slow wave: 260–460, 460–660 and 660–860 ms. The scalp maps evidenced the location of the maximum in these differences. A cluster of sensors was then generated for each patient based on these difference maps (see [Figures 1, 3, 5 and 7](#) for the extreme difference: high minus low selection).

The ERFs were averaged for each item, each time window within the cluster. These averages were exported for the selected sensor clusters and then entered into a two-way 3×3 ANOVA for each latency band, with selection demand (high, middle and low) and timing of the window (260–460, 460–660 and 660–860 ms) as factors. A correlation was performed between the averaged ERF cluster amplitude for each item and its associated ratio, thus directly contrasting the item ratio with cluster amplitude. The correlation was performed for each time window. Because we aimed to describe effects at the single-case level, each patient was analysed separately.

Source space

The cortical surface geometry from the structural MRI was obtained using Freesurfer software (Fischl, 2012) and reduced to a value close to 15,000 vertices to facilitate analyses. These cortical surfaces were aligned with the sensors attending to the digitized head points. Depth-weighted minimum norm estimate (Gramfort et al., 2013) was used to estimate the dipoles along the cortex. Depth weighting corrects the MNE bias for superficial sources (Lin et al., 2006). A noise covariance matrix was acquired based on the baselines. An overlapping spheres method was used to estimate the forward model. The dw-MNE solution was then calculated for each item and millisecond (–100 to 1000 ms) based on signed ERFs.

Item-based statistical analyses were performed using SPM12 for each patient. We performed second-level one-sample *t*-tests on the absolute source values, taking the ratio associated with each item as a covariate. The introduced contrast of interest was a negative relation between the ratio and the sources associated with each item (hence, larger absolute source amplitudes should be associated with higher selection demands – a lower ratio). The latency bands deduced from the ERFs were used as the time windows of interest for the source analyses, restricting, in this way, the possible 1000 ms source configurations.

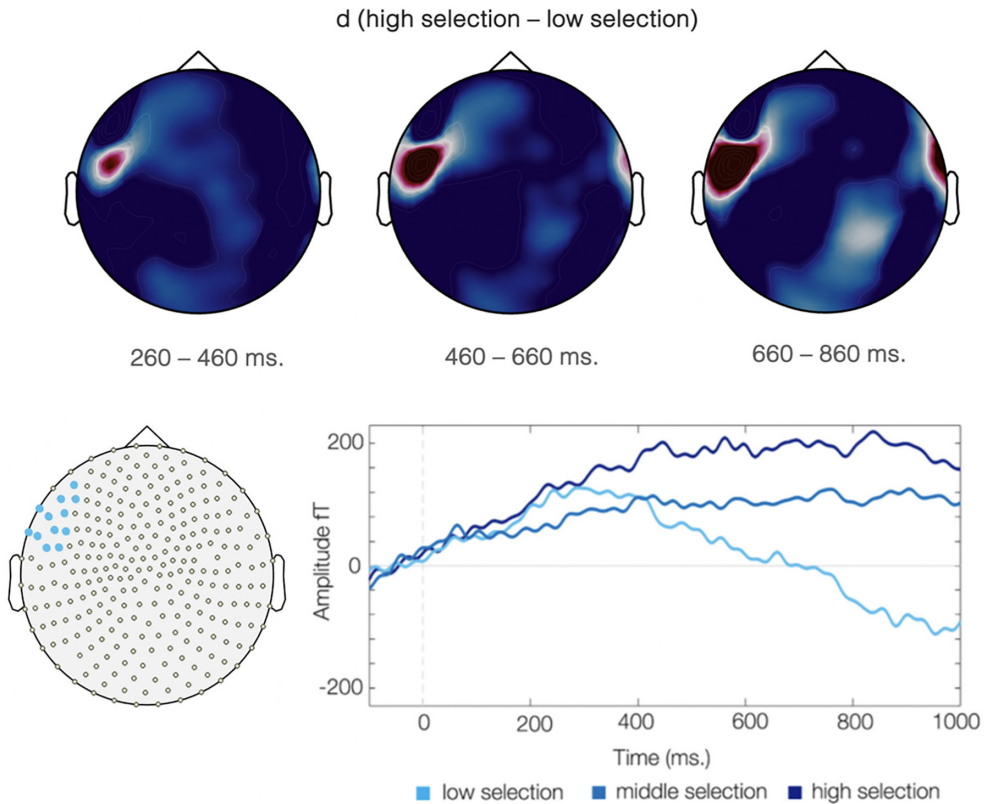


FIGURE 1 Results from Patient L at the sensor space. The ERF slow component present between 260 and 860 ms after the presentation of auditory stimulus. The amplitude of the component varied according to the degree of selection demands of the nouns, with the highest amplitude for high selection, followed by middle selection and low selection. Clear left lateralization of the patient can be observed.

RESULTS

Patient L

Sensor space

For Patient L, the visual analysis of the difference scalp map revealed maximum differences between the selection demands conditions in a left frontal cluster of sensors (Figure 1). The ANOVA confirmed a main effect of selection demands with no interaction by time window ($F(2, 288) = 4.81; p = .009$) in this cluster. The post-hoc contrast HS–LS showed a statistically significant effect (Bonferroni corrected $t = 3.094; p = .007$). The correlation analyses more precisely showed a correlation between cluster amplitudes and the selection-related ratio associated with each item, starting 460 ms after the stimulus, in the two last time windows (260–460 ms: $r = -.079$ n.s.; 460–660 ms: $r = -.211; p = .018$; 660–860 ms: $r = -.268; p = .004$). The negative correlation involved higher amplitudes of the (positive) slow wave as the ratio decreased (higher demands).

Source space

The t-tests conducted for each window revealed the strongest effect of selection demand in the 460–660 for Patient L. Significant brain sources (p corrected $< .038$) were localized mainly in BA 44 and BA 45 (Figure 2). The activation intensity in BA 44 and BA 45 increased according to selection demand (lower ratios – larger source intensities). During the last time window (660–860 ms), again significant sources were shown in the IFG, yet more anteriorly (orbital gyrus).

Patient A

Sensor space

Like Patient L, the visual analysis of the difference scalp in A showed differences between the selection demand conditions in frontal sensors (Figure 3). The ANOVA showed a main effect of selection demands, with no interaction by time window ($F(2, 156) = 12.23; p < .001$), in a left frontal cluster. The post-hoc contrast showed a statistical difference between HS and LS (Bonferroni corrected, $t = 3.099; p < .001$) and MS and LS (Bonferroni corrected $t = 3.45; p = .002$). A significant correlation appeared between the cluster amplitudes and the selection-related ratio associated with each item from 460 ms in the two last time windows (260–460 ms: $r = -.18$ n.s.; 460–660 ms: $r = -.42; p < .001$; 660–860 ms: $r = -.28; p = .019$). Again, the negative correlation implied higher amplitudes as the ratio decreased (higher demands).

Source space

For Patient A, significant sources (p corrected $< .01$) were detected in the first two windows. Source intensity in the left BA 45 (pars triangularis) significantly increased as selection demands increased (Figure 4) from 260 to 460 ms after the noun. Only between 260 and 460 ms significant selection-related activation was also found in the left rostral middle frontal gyrus. Again, the left IFG source amplitudes

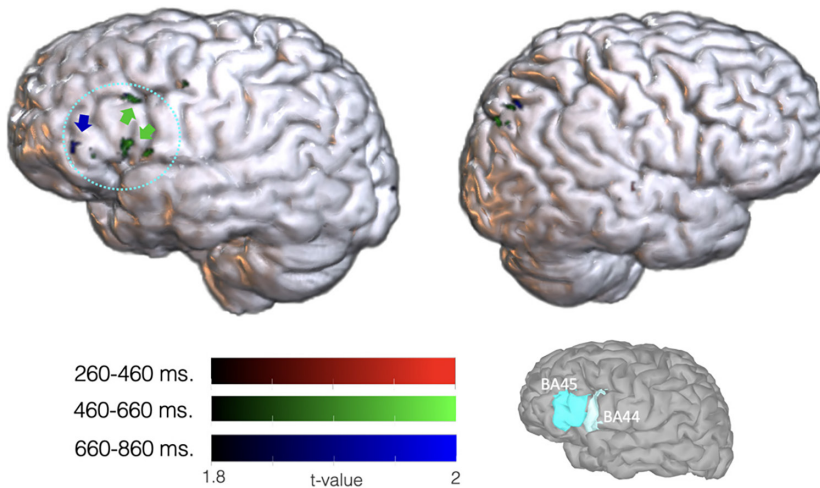


FIGURE 2 Results from Patient L at the source space for the selection contrasts, with colours representing different time windows (corrected $p < .038$). Left BA44 and BA45 are depicted according to the Freesurfer reconstructed atlas for the patient.

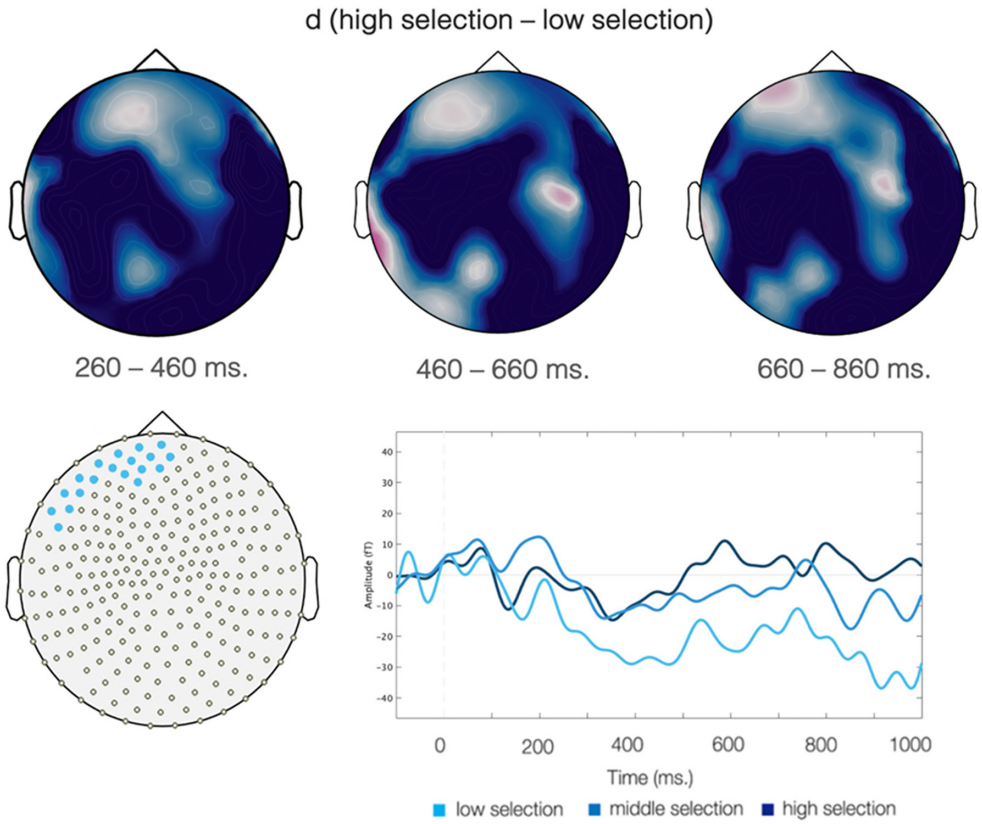


FIGURE 3 Results from Patient A at the sensor space. Starting from 260ms, the amplitude of the ERFs was modulated by the selection demand imposed by the noun. The detected cluster extended over left frontal areas.

were sustainedly and negatively associated with the selection ratio covariable (lower ratios/higher demand and larger source intensities).

Patient S

Sensor space

For Patient S, the visual analysis of the difference scalp map revealed maximum differences between the selection demand conditions in a right frontal cluster of sensors (Figure 5). The ANOVA confirmed a main effect of selection demands with no interaction by time window ($F(2,192) = 24.37$; $p < .001$) in this cluster. The post-hoc contrast HS–LS showed a statistically significant effect (Bonferroni corrected $t = -6.91$; $p < .001$), as well as the HS–MS ($t = -2.65$; $p = .026$) and MS–LS contrasts ($t = -4.34$; $p = .001$). The correlation analyses more precisely showed a correlation between cluster amplitudes and the selection-related ratio associated with each item in all the time windows (260–460ms: $r = .43$; $p < .001$; 460–660ms: $r = .43$; $p < .001$; 660–860ms: $r = .38$; $p < .001$). The positive correlation involved higher amplitudes of the (negative) slow wave as the ratio decreased.

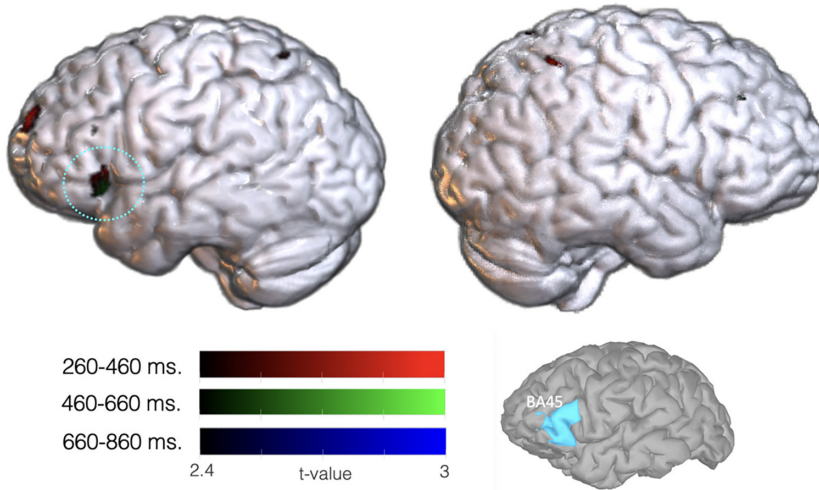


FIGURE 4 Results from Patient A at the source space for the selection contrasts, with colours representing different time windows (corrected $p < .01$). Left BA45 is depicted according to the Freesurfer reconstructed atlas for the patient.

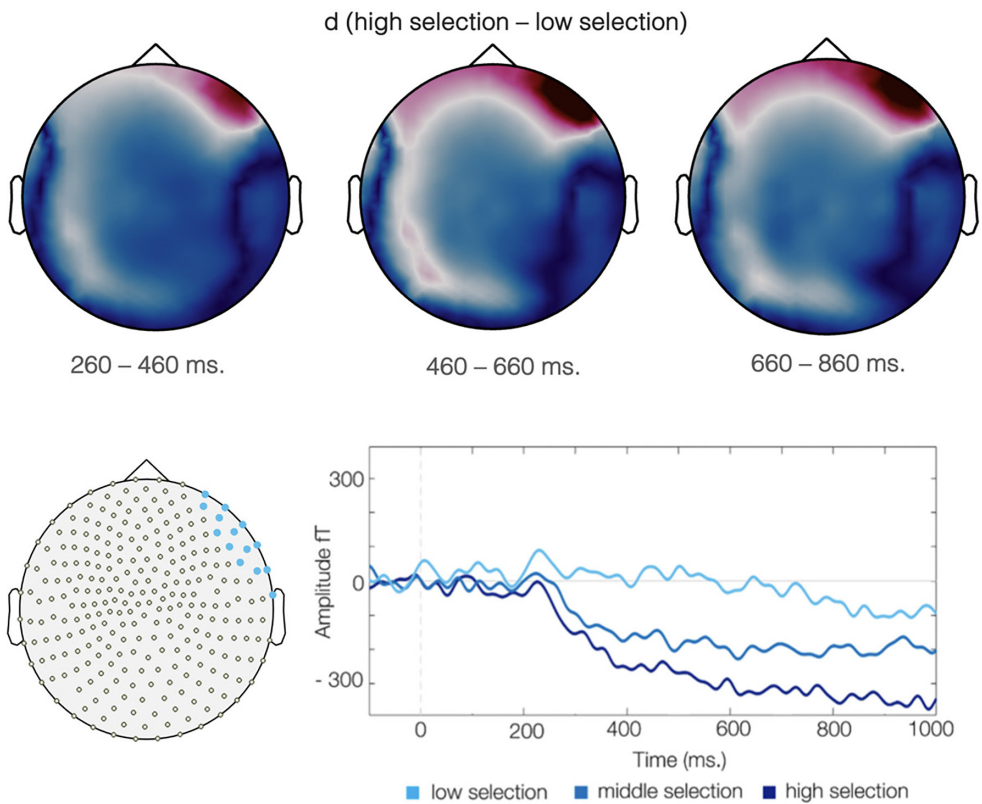


FIGURE 5 Results from Patient S at the sensor space – Differences across the three conditions in the slow component starting at 260–860ms after the cue signalling emission of the verb. Comparing to the other patients, this patient exhibited an earlier MS-LS effect, so all the contrast effects started approximately at the same latency (~260ms). Activation varied along the degree of selection demands of the nouns, with the highest amplitude for high selection, followed by middle selection and low selection. Importantly, right lateralization appears in the maximum differences, which can be due to reorganization.

Source space

Like Patient L, the *t*-tests conducted for each window revealed the strongest effect of selection demand in the 460–660 for Patient S. The source estimation based on the ERFs showed the highest and focal activation most visible in the right BA 45. There were also minor activations in the right BA 47 and right temporal pole and the left hemisphere in the superior and middle frontal gyrus (Figure 6). The activation intensity in these areas was increased according to selection demand with higher activation as selection demand increased (lower ratios). Therefore, a negative correlation between selection conditions and activation of these areas is present (negative relationship tested, hence positive *t*-values). The observed strong effect in the right IFG and the lack of activation in the left IFG could have been induced by reorganization due to early-onset epilepsy. It still should be noted that there are minor residual activations in the more superior part of the left frontal lobe.

Patient G

Sensor space

The visual inspection of the difference scalp maps for this patient revealed differences between HS and MS conditions, but the difference was not so evident for the MS-LS subtraction (Figure 7). Effects were detected in a small left-hemisphere cluster and a more extensive right-hemisphere cluster. Hence, for the left-hemisphere cluster, the ANOVA showed a main effect of selection demands with no interaction by time window ($F(2,174) = 10.159$; $p < .001$). Post-hoc analysis showed that the HS differed from LS (Bonferroni corrected $t = 4.101$; $p < .001$) and from MS ($t = 3.39$; $p = .003$). Correlational analysis showed a negative correlation between the selection-related ratio and the cluster amplitude from the first window (260–460 ms: $r = -.25$; $p < .051$; 460–660 ms: $r = -.28$; $p = .029$; 660–860 ms: $r = -.27$; $p = .039$).

The right frontal cluster was larger in extension, and again, the ANOVA revealed a main effect of selection demands with no interaction by window ($F(2,174) = 7.193$; $p < .001$). Post-hoc contrast showed marginal differences between HS-LS (Bonferroni corrected, $t = 2.31$; $p = .06$) and between HS-MS ($t = 3.69$; $p < .001$). The correlational analyses revealed a negative correlation between the selection-related ratio and the cluster amplitude from 460 ms in the two last time windows (460–660 ms: $r = .22$;

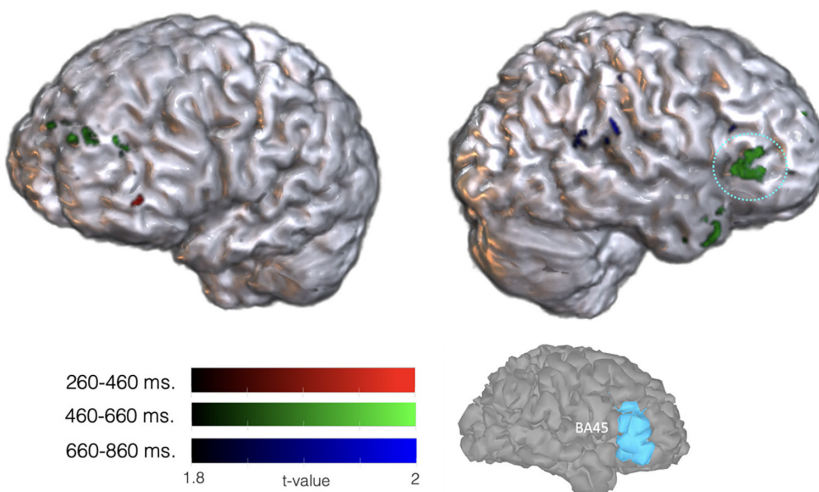


FIGURE 6 Results from Patient S at the source space for the selection contrasts, with colours representing different time windows (corrected $p < .038$). Right BA45 is depicted according to the Freesurfer reconstructed atlas for the patient.

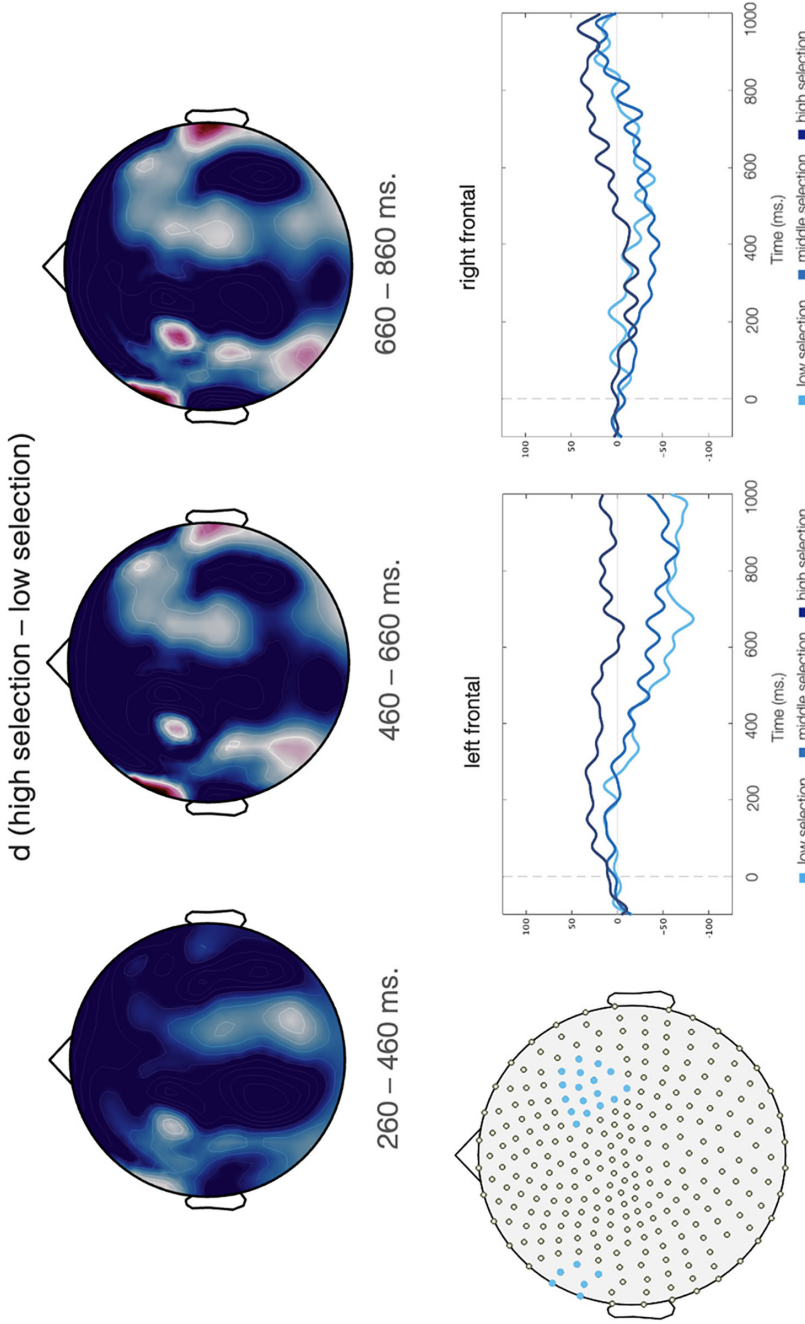


FIGURE 7 Results from Patient G at the sensor space. Two clusters were selected for analyses, in left and right anterior zones. While in the left cluster, the effects started at 260 ms. Effects in the right cluster were evident from 460 ms.

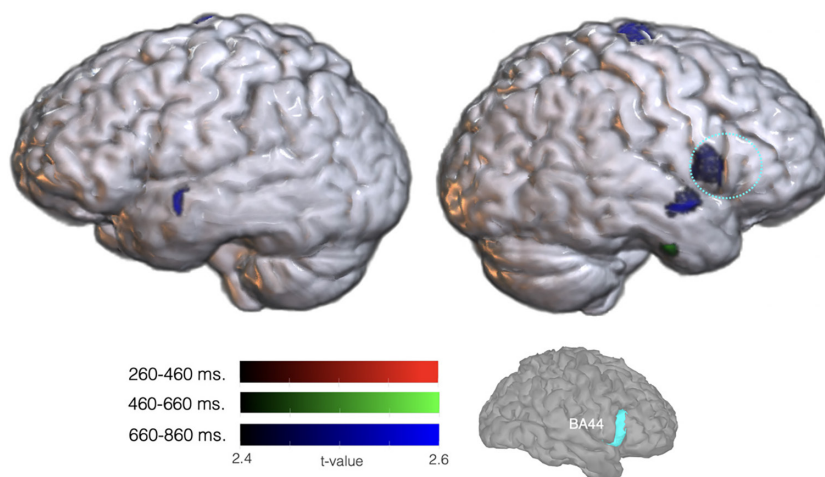


FIGURE 8 Results from Patient G at the source space for the selection contrasts, with colours representing different time windows (corrected $p < .01$). The main effects appear at the right inferior fronto-temporal areas. Right BA44 is depicted according to the Freesurfer reconstructed atlas for the patient.

$p = .04$; 660–860 ms: $r = .23$; $p = .035$). The negative correlation means higher amplitudes for higher selection demands as the ratio decreases (higher demands).

Source space

The t -test on the source amplitudes showed significant activations between 660 and 860 ms after the noun. Again, significant ratio effects appeared most extensively in the IFG, specifically in the right BA 44 (pars opercularis) and the superior temporal gyrus. Effects were also found in the caudal superior frontal gyrus, with less extension in the left superior temporal gyrus (Figure 8). Therefore, like in S, we observed a shift in the verb selection-related effect to the contralateral homologue of Broca's area.

DISCUSSION

The present study aimed to provide focal localization of frontal language-related areas at the individual case level. It sought to adapt the common verb generation task to make the test more specific. Besides, the adaptation must be sensitive to reorganization since the task detects functionally equivalent recruited areas. It must also be sensitive to right language lateralization.

In line with our hypothesis, MEG showed ERF effects with an adapted version of the verb generation task. Using the ratio of selection demands of the nouns as a contrast led to a linear relation between ERFs amplitudes and selection level. This adaptation of the commonly used verb generation task also yielded precise detection of lateralization among patients, including right lateralization.

ERFs varied in terms of the polarity for Patient S, yet the functional meaning of the slow wave in the four patients appeared to be the same: The positive/negative amplitude linearly depended on the associated ratio. On the other hand, verb selection demands were linearly related to source amplitudes in the IFG in all patients.

This role of IFG, which is not retrieval from semantic knowledge *per se*, but a selection among alternatives (Thompson-Schill et al., 1997, 1998), serves in our study as a practical application to localize a known linguistic function of the IFG with higher precision. An easy methodological variation of the

verb generation task, which is applying the selection ratio to nouns, could provide higher accuracy to the presurgical mapping of the frontal lobe.

Another input of the present study is that the item classification worked with different sets of stimuli. Three slightly different verb generation tasks were applied. Yet, in all cases, we observed the expected effects. This validates the current analysis; hence, the classification used here could be applied to further sets of stimuli, including different nouns. It implies a ranking across items and a correlation index with the actual ratio given for each noun, which derives from differential IFG involvement.

Mapping IFG before surgery is crucial, given that this region has an indisputable role in language. It is recruited in phonological and semantic processes in a general sense (Klaus & Hartwigsen, 2019), as well as in syntactic processing (Caplan et al., 2008; Roöder et al., 2002), grammar learning (Pettersson et al., 2004) and verbal working memory (Makuuchi et al., 2009). Our study might help in the amount of focality achieved during IFG mapping. We detected small and focal areas involved in the post-retrieval selection of semantic knowledge, in which activation depended on the noun selection demands. The detected focal regions may provide the surgeon with a broader scope for the resection if needed.

With this manipulation of the verb generation task, our second aim was to be able to detect right lateralization. Given that the verb generation task is already validated for lateralization and found concordant results across studies (Bowyer et al., 2005; Findlay et al., 2012; Gaillard et al., 2002), the manipulation employed in the current analysis could lead to better discrimination in terms of hemispheric lateralization. Patient S had early-onset epilepsy, and although most of the population is left lateralized in terms of language, epilepsy patients can develop an atypical language organization (Hamberger & Cole, 2011). Disruption of the typical organization of language by epilepsy might have induced this patient's right reorganization. Since epilepsy does not imply sudden damage as stroke or trauma but instead causes a progressive disruption of language function, a shift to the right hemisphere is probable in this condition, especially with an early epilepsy onset (Janszky et al., 2006; Lidzba et al., 2017). Identifying the lateralization is crucial due to possible neurosurgery in refractory epilepsy. Therefore, detecting a patient's language function with the current task is important and informs about language reorganization in epilepsy. Beyond discerning between reorganization and lateralization, the paradigm can precisely detect activations in the relevant brain hemisphere.

Similarly, in Patient G, we found a predominance of the right IFG responding to verb selection demands. It is well known that the slow growth of low-grade gliomas can lead to neural reorganization. Slow-growing LGG explains the preservation of cognitive function despite the involvement of the so-called eloquent structures. In G, the left temporal lobe was affected. These lesions induce progressive brain reshaping (Duffau, 2015). Data suggest that a network of areas might have been recruited contralaterally, including IFG areas. This patient underwent DES stimulation during surgery, showing no positives and no language deficit pre- or post-surgery. Hence, in two cases, we detect reorganization with focality in the IFG, and we show the potential of contralateral sites for carrying the default role of the left IFG.

As further development from the present study, these results could guide direct electrical cortical stimulation (DES). DES applies electrical stimuli to inhibit or excite function. Verb generation tasks are commonly used during electrostimulation in awake surgery (Black et al., 2017; Ruis, 2018). The present results prompt the consideration of the nouns used during stimulation. With a good selection of the eliciting nouns or pictures to use during DES mapping, we should avoid false negatives and increase sensitivity during IFG stimulation. If this characteristic of the items is not considered and stimuli requiring very-low-selection demands are used, there might be a high probability of obtaining a false negative. The same stimulation site could result in positive or negative depending on the concrete stimulus that has been presented, even using the same task. A possibility for optimized stimuli should involve low- or medium-selection nouns. Further research is needed to set such a set of stimuli for VG during DES.

Here, MEG was employed as the neuroimaging technique, allowing us to see the effect of selection demand on the verb generation task with very high temporal resolution. Thanks to it, we could indicate the effect of selection demands, which started at 260–460 ms after the noun and reached the strongest at 460–660 ms after. In contrast to fMRI, in the case of tumours, the BOLD response in neighbour areas of a tumour might not demonstrate the neural activity as accurately (Roux et al., 2003). This decreased sensitivity does not seem to reflect diminished neural activity but rather derives from a change in the

neurovascular and metabolic coupling (Aubert et al., 2002). As another whole-brain mapping technique (but see comparison with stimulation techniques in Tarapore et al., 2013), MEG does not show this decreased sensitivity due to a direct measure of neural activity rather than relying on metabolic changes in the brain.

However, and attending to the shape of the ERFs effects, it must be pointed out that the manipulated variable in the present study yielded a sustained slow wave. This, in turn, implies that it is very likely that a technique with less temporal resolution, such as fMRI, should show similar effects. As can be seen in the results, the effect of selection demand on the verb generation task gives rise to a slow component, which is present from 260 to 460 ms time window up to 1000 ms. This long time would be enough for fMRI temporal resolution to detect the effect. The slow component indicates that this variation in the verb generation task can be applied to fMRI and MEG.

Overall, and despite the known limitations inherent to any case report, the present study stresses the relevance of adapting neuroimaging paradigms used for presurgical mapping in a way that we can combine the description of the whole network for language functions but also dissect the network in its components. Lexical selection is one example of how this could be done. Other tasks, such as object naming, or even more complex tasks, such as sentence production, could be adapted as well. The accepted neuroimaging paradigms within a given hospital probably do not need too many modifications. There is long-time knowledge in cognitive neuroscience about the processes behind the most frequently used tasks, and highly likely, cognitive neuroscience can inform presurgical mapping on what specific items should be emphasized for a given brain area.

AUTHOR CONTRIBUTIONS

Conceptualization: E.S. and C.S.; Investigation: E.S., E.N.V., G.A., D.D.A. and C.L. Formal Analysis: E.S.; Funding Acquisition: E.S. and C.S.; Writing – Original Draft Preparation: E.S.; and Writing – Review and Editing: E.S. and C.S.

ACKNOWLEDGEMENTS

The European Union's Horizon 2020 research and innovation programme under the Marie Skłodowska-Curie grant agreement No. 793071 to E.S.

CONFLICT OF INTEREST STATEMENT

The authors have no conflicts of interest to declare.

DATA AVAILABILITY STATEMENT

Data will be available upon request to the authors, according to Italian regulations.

ORCID

Elena Salillas  <https://orcid.org/0000-0002-0873-5357>

REFERENCES

- Allendorfer, J. B., Lindsell, C. J., Siegel, M., Banks, C. L., Vannest, J., Holland, S. K., & Szaflarski, J. P. (2012). Females and males are highly similar in language performance and cortical activation patterns during verb generation. *Cortex*, 48(9), 1218–1233. <https://doi.org/10.1016/J.CORTEX.2011.05.014>
- Aubert, A., Costalat, R., Duffau, H., & Benali, H. (2002). Modeling of pathophysiological coupling between brain electrical activation, energy metabolism and hemodynamics: Insights for interpreting intracerebral tumor imaging. *Acta Biotheoretica*, 50(4), 281–295. <https://doi.org/10.1023/A:1022620818701/METRICS>
- Bastiaanse, R., & Jonkers, R. (2007). Verb retrieval in action naming and spontaneous speech in agrammatic and anomic aphasia. *Aphasiology*, 12(11), 951–969. <https://doi.org/10.1080/02687039808249463>
- Black, D. F., Vachha, B., Mian, A., Faro, S. H., Maheshwari, M., Sair, H. I., Petrella, J. R., Pillai, J. J., & Welker, K. (2017). American Society of Functional Neuroradiology—Recommended fMRI paradigm algorithms for presurgical language assessment. *American Journal of Neuroradiology*, 38(10), E65–E73. <https://doi.org/10.3174/AJNR.A5345>

- Bowyer, S. M., Moran, J. E., Weiland, B. J., Mason, K. M., Greenwald, M. L., Smith, B. J., Barkley, G. L., & Tepley, N. (2005). Language laterality determined by MEG mapping with MR-FOCUSS. *Epilepsy and Behavior*, *6*(2), 235–241. <https://doi.org/10.1016/J.YEBEH.2004.12.002>
- Caplan, D., Chen, E., & Waters, G. (2008). Task-dependent and task-independent neurovascular responses to syntactic processing. *Cortex*, *44*(3), 257–275. <https://doi.org/10.1016/J.CORTEX.2006.06.005>
- Cerliani, L., Thomas, R. M., Aquino, D., Contarino, V., & Bizzi, A. (2016). Disentangling subgroups of participants recruiting shared as well as different brain regions for the execution of the verb generation task: A data-driven fMRI study. *Cortex*, *86*, 247–259. <https://doi.org/10.1016/J.CORTEX.2016.11.017>
- Cirillo, S., Battistella, G., Castellano, A., Sanvito, F., Iadanza, A., Bailo, M., Barzaghi, R. L., Acerno, S., Mortini, P., Gorno-Tempini, M. L., Mandelli, M. L., & Falini, A. (2022). Comparison between inferior frontal gyrus intrinsic connectivity network and verb-generation task fMRI network for presurgical language mapping in healthy controls and in glioma patients. *Brain Imaging and Behavior*, *16*(6), 2569–2585. <https://doi.org/10.1007/S11682-022-00712-Y>
- Damasio, A. R., & Tranel, D. (1993). Nouns and verbs are retrieved with differently distributed neural systems. *Proceedings of the National Academy of Sciences*, *90*(11), 4957–4960. <https://doi.org/10.1073/PNAS.90.11.4957>
- Duffau, H. (2015). Plasticity of cognition in brain gliomas. In J. I. Tracy, B. Hampstead, & K. Sathian (Eds.), *Cognitive plasticity in neurologic disorders*. Oxford University Press.
- Findlay, A. M., Ambrose, J. B., Cahn-Weiner, D. A., Houde, J. F., Honma, S., Hinkley, L. B. N., Berger, M. S., Nagarajan, S. S., & Kirsch, H. E. (2012). Dynamics of hemispheric dominance for language assessed by magnetoencephalographic imaging. *Annals of Neurology*, *71*(5), 668–686. <https://doi.org/10.1002/ANA.23530>
- Fischl, B. (2012). FreeSurfer. *NeuroImage*, *62*(2), 774–781. <https://doi.org/10.1016/J.NEUROIMAGE.2012.01.021>
- Gaillard, W. D., Balsamo, L., Xu, B., Grandin, C. B., Braniecki, S. H., Papero, P. H., Weinstein, S., Conry, J., Pearl, P. L., Sachs, B., Sato, S., Jabbari, B., Vezina, L. G., Frattali, C., & Theodore, W. H. (2002). Language dominance in partial epilepsy patients identified with an fMRI reading task. *Neurology*, *59*(2), 256–265. <https://doi.org/10.1212/WNL.59.2.256>
- Gramfort, A., Luessi, M., Larson, E., Engemann, D. A., Strohmeier, D., Brodbeck, C., Goj, R., Jas, M., Brooks, T., Parkkonen, L., & Hämäläinen, M. (2013). MEG and EEG data analysis with MNE-python. *Frontiers in Neuroscience*, *7*(7), 267. <https://doi.org/10.3389/FNINS.2013.00267/BIBTEX>
- Grè, J., & Decety, J. (2001). Functional anatomy of execution, mental simulation, observation, and verb generation of actions: A meta-analysis †. *Human Brain Mapping*, *12*, 1–19. <https://doi.org/10.1002/1097-0193>
- Hamberger, M. J., & Cole, J. (2011). Language organization and reorganization in epilepsy. *Neuropsychology Review*, *21*(3), 240–251. <https://doi.org/10.1007/S11065-011-9180-Z/FIGURES/1>
- Janszky, J., Mertens, M., Janszky, I., Ebner, A., & Woermann, F. G. (2006). Left-sided interictal epileptic activity induces shift of language lateralization in temporal lobe epilepsy: An fMRI study. *Epilepsia*, *47*(5), 921–927. <https://doi.org/10.1111/J.1528-1167.2006.00514.X>
- Klaus, J., & Hartwigsen, G. (2019). Dissociating semantic and phonological contributions of the left inferior frontal gyrus to language production. *Human Brain Mapping*, *40*(11), 3279–3287. <https://doi.org/10.1002/HBM.24597>
- Laudanna, A., Thornton, A., Brown, G., Burani, C., & Marconi, L. (1995). Un corpus dell'italiano scritto contemporaneo dalla parte del ricevente. In S. Bolasco, L. Lebart, & A. Salem (Eds.), *III Giornate Internazionali Di Analisi Statistica Dei Dati Testuali* (Vol. I, pp. 103–109). Cisu.
- Lidzba, K., Küpper, H., Kluger, G., & Staudt, M. (2017). The time window for successful right-hemispheric language reorganization in children. *European Journal of Paediatric Neurology: EJPN*, *21*(5), 715–721. <https://doi.org/10.1016/J.EJPN.2017.06.001>
- Lin, F. H., Witzel, T., Ahlfors, S. P., Stufflebeam, S. M., Belliveau, J. W., & Hämäläinen, M. S. (2006). Assessing and improving the spatial accuracy in MEG source localization by depth-weighted minimum-norm estimates. *NeuroImage*, *31*(1), 160–171. <https://doi.org/10.1016/J.NEUROIMAGE.2005.11.054>
- Makuuchi, M., Bahlmann, J., Anwender, A., & Friederici, A. D. (2009). Segregating the core computational faculty of human language from working memory. *Proceedings of the National Academy of Sciences of the United States of America*, *106*(20), 8362–8367. https://doi.org/10.1073/PNAS.0810928106/SUPPL_FILE/0810928106SL.PDF
- Martin, R. C., & Yan, C. (2006). Selection demands versus association strength in the verb generation task. *Psychonomic Bulletin and Review*, *13*(3), 396–401. <https://doi.org/10.3758/BF03193859/METRICS>
- Mätzig, S., Druks, J., Masterson, J., & Vigliocco, G. (2009). Noun and verb differences in picture naming: Past studies and new evidence. *Cortex*, *45*(6), 738–758. <https://doi.org/10.1016/J.CORTEX.2008.10.003>
- Miceli, G., Silveri, M. C., Nocentini, U., & Caramazza, A. (2007). Patterns of dissociation in comprehension and production of nouns and verbs. *Aphasiology*, *23*(3–4), 351–358. <https://doi.org/10.1080/02687038808248937>
- Pang, E. W., Wang, F., Malone, M., Kadis, D. S., & Donner, E. J. (2011). Localization of Broca's area using verb generation tasks in the MEG: Validation against fMRI. *Neuroscience Letters*, *490*(3), 215–219. <https://doi.org/10.1016/J.NEULET.2010.12.055>
- Peirce, J. W. (2007). PsychoPy—Psychophysics software in python. *Journal of Neuroscience Methods*, *162*(1–2), 8–13. <https://doi.org/10.1016/J.JNEUMETH.2006.11.017>
- Petersson, K. M., Forkstam, C., & Ingvar, M. (2004). Artificial syntactic violations activate Broca's region. *Cognitive Science*, *28*(3), 383–407. <https://doi.org/10.1016/J.COGSCI.2003.12.003>
- Pillon, A., & d'Honinchtun, P. (2011). The organization of the conceptual system: The case of the "object versus action" dimension. *Cognitive Neuropsychology*, *27*(7), 587–613. <https://doi.org/10.1080/02643294.2011.609652>

- Rofes, A., & Miceli, G. (2014). Language mapping with verbs and sentences in awake surgery: A review. *Neuropsychology Review*, 24(2), 185–199. <https://doi.org/10.1007/S11065-014-9258-5/TABLES/3>
- Roöder, B., Stock, O., Neville, H., Bien, S., & Röslér, F. (2002). Brain activation modulated by the comprehension of normal and pseudo-word sentences of different processing demands: A functional magnetic resonance imaging study. *NeuroImage*, 15(4), 1003–1014. <https://doi.org/10.1006/NIMG.2001.1026>
- Roux, F. E., Boulanouar, K., Lotteric, J. A., Mejdoubi, M., LeSage, J. P., Berry, I., Berger, M. S., McKhann, G. M., Hirsch, J., & Schramm, J. (2003). Language functional magnetic resonance imaging in preoperative assessment of language areas: Correlation with direct cortical stimulation. *Neurosurgery*, 52(6), 1335–1347. <https://doi.org/10.1227/01.NEU.0000064803.05077.40>
- Ruis, C. (2018). Monitoring cognition during awake brain surgery in adults: A systematic review. *Journal of Clinical and Experimental Neuropsychology*, 40(10), 1081–1104. <https://doi.org/10.1080/13803395.2018.1469602>
- Shapiro, K., & Caramazza, A. (2003). Grammatical processing of nouns and verbs in left frontal cortex? *Neuropsychologia*, 41(9), 1189–1198. [https://doi.org/10.1016/S0028-3932\(03\)00037-X](https://doi.org/10.1016/S0028-3932(03)00037-X)
- Tadel, F., Baillet, S., Mosher, J. C., Pantazis, D., & Leahy, R. M. (2011). Brainstorm: A user-friendly application for MEG/EEG analysis. *Computational Intelligence and Neuroscience*, 2011, 879716. <https://doi.org/10.1155/2011/879716>
- Tarapore, P. E., Findlay, A. M., Honma, S. M., Mizuir, D., Houde, J. F., Berger, M. S., & Nagarajan, S. S. (2013). Language mapping with navigated repetitive TMS: Proof of technique and validation. *NeuroImage*, 82, 260–272. <https://doi.org/10.1016/j.neuroimage.2013.05.018>
- The MathWorks Inc. (2022). *MATLAB version: 9.13.0 (R2022b)*. The MathWorks Inc. <https://www.mathworks.com>
- Thompson-Schill, S. L., D'Esposito, M., Aguirre, G. K., & Farah, M. J. (1997). Role of left inferior prefrontal cortex in retrieval of semantic knowledge: A reevaluation. *Proceedings of the National Academy of Sciences of the United States of America*, 94(26), 14792–14797. <https://doi.org/10.1073/PNAS.94.26.14792/ASSET/BC7B48CE-0EBF-498F-B590-4E89DAD4959E/ASSETS/GRAPHIC/PQ2673655003.JPEG>
- Thompson-Schill, S. L., Swick, D., Farah, M. J., D'Esposito, M., Kan, I. P., & Knight, R. T. (1998). Verb generation in patients with focal frontal lesions: A neuropsychological test of neuroimaging findings. *Proceedings of the National Academy of Sciences of the United States of America*, 95(26), 15855–15860. <https://doi.org/10.1073/PNAS.95.26.15855>
- Tracy, J. I., & Osipowicz, K. Z. (2011). A conceptual framework for interpreting neuroimaging studies of brain neuroplasticity and cognitive recovery. *NeuroRehabilitation*, 29(4), 331–338. <https://doi.org/10.3233/NRE-2011-0709>
- Wagner, A. D., Paré-Blagoev, E. J., Clark, J., & Poldrack, R. A. (2001). Recovering meaning: Left prefrontal cortex guides controlled semantic retrieval. *Neuron*, 31(2), 329–338. [https://doi.org/10.1016/S0896-6273\(01\)00359-2](https://doi.org/10.1016/S0896-6273(01)00359-2)

How to cite this article: Salillas, E., Luisi, C., Arcara, G., Varlı, E. N., d'Avella, D., & Semenza, C. (2023). Verb generation for presurgical mapping: Gaining specificity. *Journal of Neuropsychology*, 00, 1–22. <https://doi.org/10.1111/jnp.12355>

APPENDIX A

Set of nouns and ratios for each patient

Item	Ratio
Items for L, G and A	
ragno	1,0
torre	1,0
denti	1,0
divano	1,0
bottone	1,0
bocca	1,0
sole	1,0
pera	1,0
nasò	1,0
furgone	1,0

Item	Ratio
lampada	1,1
dado	1,2
profumo	1,2
cascata	1,3
chiodo	1,3
spada	1,3
microfono	1,3
orologio	1,3
anello	1,3
cacciavite	1,3
fuoco	1,4
chiave	1,4
gomma	1,4
fiore	1,5
fionda	1,5
ape	1,6
cassetto	1,6
noce	1,7
osso	1,7
luna	1,8
carota	1,8
cipolla	1,8
specchio	1,8
occhiali	1,8
mucca	1,8
vulcano	1,8
forno	2,0
corvo	2,0
ascia	2,0
calzini	2,0
banconote	2,0
mano	2,0
palla	2,0
pentola	2,0
mosca	2,2
padella	2,3
camicia	2,3
zanzara	2,3
casa	2,3
arancia	2,3
vite	2,7
lingua	2,7
gonna	2,7
gamba	2,7

Item	Ratio
giacca	2,8
martello	3,0
colla	3,0
mela	3,0
telefono	3,0
onda	3,0
vespa	3,0
braccio	3,0
scudo	3,3
piede	3,5
treno	3,5
arco	3,5
rosa	4,0
armadio	4,0
sci	4,3
fragola	4,5
flauto	5,0
scarpa	5,0
cavallo	5,5
uva	5,5
bicchiere	5,5
unghia	6,0
collana	6,0
letto	6,0
timbro	6,0
barca	6,5
anguria	6,5
sapone	6,5
faro	6,5
maracas	7,0
automobile	7,0
porta	7,5
gatto	7,5
tigre	9,0
mare	10,0
gallo	14,0
pettine	16,0
coltello	16,0
tazza	16,0
arpa	16,0
bilancia	17,0
penna	17,0
aereo	17,0
pistola	17,0

Item	Ratio
forbici	17,0
sedia	18,0
Items for S	
sole	1,0
occhi	1,0
mucca	1,0
stadio	1,0
pugno	1,0
ago	1,0
naso	1,0
miele	1,0
sasso	1,0
vite	1,0
velo	1,0
scudo	1,3
spugna	1,3
chiave	1,3
dado	1,3
gabbia	1,3
ape	1,3
laccio	1,3
piuma	1,3
tappo	1,3
rose	1,5
pioggia	1,5
scimmia	1,5
ghiaccio	1,5
torre	1,5
nave	1,5
zebra	1,5
pancia	1,5
onda	1,5
torta	1,7
baffi	1,7
arco	1,7
barca	1,7
lingua	1,7
auto	1,8
sveglia	2,0
palla	2,0
frutta	2,0
mano	2,0
unghie	2,0
borsa	2,0

Item	Ratio
testa	2,0
calze	2,0
gonna	2,0
lente	2,0
treno	2,0
denti	2,0
forno	2,0
vaso	2,0
bruco	2,3
cielo	2,3
soldi	2,3
remo	2,5
fumo	2,5
aglio	2,5
zucca	2,5
braccio	2,5
fiore	2,5
filo	2,7
fetta	3,0
pozzo	3,0
riso	3,0
gatto	3,0
mela	3,5
corda	3,5
bocca	3,5
tigre	4,0
porta	4,0
sposa	4,0
erba	4,0
pepe	4,0
olio	4,0
succo	4,0
vino	6,0
gioco	6,0
pizza	7,0
caffè	7,0
casa	7,0
prugna	8,0
fuoco	8,0
cane	8,0
notte	8,0
fiume	8,0
latte	8,0
gomma	9,0

Item	Ratio
tasto	9,0
vento	9,0
cuore	9,0
giacca	9,0
ladro	10,0
sedia	10,0
cuoco	10,0
letto	11,0
pinne	11,0
ali	11,0
piedi	11,0
penna	12,0
tromba	12,0
radio	12,0
libro	12,0